Numerical insights into turbulent penetrative convection over localized heat sources

KenjereS, S.; Zilić, A.; Hanjalić, K.

DOI
10.1088/1742-6596/2766/1/012055

Publication date
2024

Document Version
Final published version

Published in
Journal of Physics: Conference Series

Journal of Physics: Conference Series

PAPER • OPEN ACCESS

Numerical insights into turbulent penetrative convection over localized heat sources

To cite this article: S Kenjereš *et al* 2024 *J. Phys.: Conf. Ser.* **2766** 012055

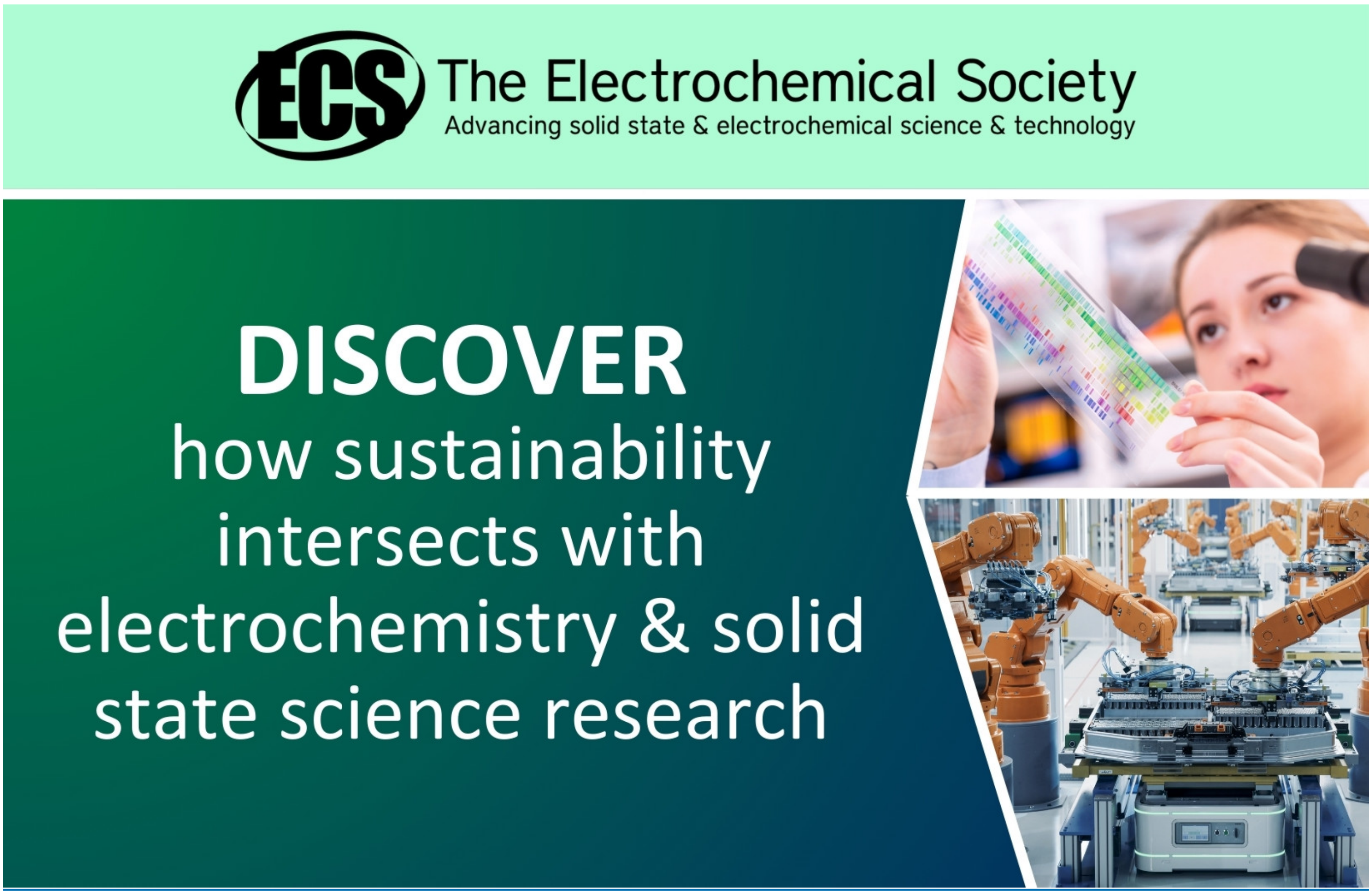

Journal of Physics: Conference Series **2766** (2024) 012055 doi:10.1088/1742-6596/2766/1/012055

Numerical insights into turbulent penetrative convection over localized heat sources

S Kenjereš, A Žilić and K Hanjalić

Department of Chemical Engineering, Faculty of Applied Sciences, Delft University of Technology, Van der Maasweg 9, 2629 HZ Delft, The Netherlands

E-mail: `s.kenjeres@tudelft.nl`

Abstract. The turbulent penetrative convection into a stable convective boundary layer represents an important phenomenon in environmental engineering and atmospheric science. In the present study, we present a series of numerical simulations performed by two modeling approaches: the high-fidelity Large-Eddy Simulations (LES), and the less computationally demanding transient Reynolds-Averaged Approach (TRANS), but with an advanced sub-scale turbulent heat flux model. By simulating different localized heat sources over the ground, and by performing a direct comparative assessment of results obtained by LES and TRANS, we confirmed an overall good agreement in predicting the time evolution of the horizontally averaged temperature profiles. Similarly, the morphology of instantaneous thermal plumes and large convective structures predicted by TRANS were in reasonable agreement with the referent LES predictions.

1. Introduction

The penetrative convection describes the vertical heat flux transport in an initially stably thermally stratified environment, [1–9]. This situation is typical for the onset of the early morning heating of the earths surface caused by incoming solar radiation. In the present study, we focus on performing a series of numerical simulations over a range of various localized heat sources (with different strengths of heating and shapes of heat source) for different scenarios of the initially stable thermal stratification. To model turbulence effects, we apply two approaches: (i) the wall-resolving large eddy simulation (LES) with a non-isotropic filtering approach to represent the sub-grid turbulence, and (ii) the time-dependent Reynolds-Averaged Navier-Stokes (TRANS) with the algebraic form of the non-isotropic turbulent heat flux model (AFM) embedded into the three-equation ($k - \varepsilon - \overline{\theta^2}$) scheme that accounts for the dynamics of the fluctuating temperature and its effect on heat transfer. The research objective is to perform a direct comparison between the referent wall-resolved high-fidelity LES and TRANS with AFM sub-scale model on a much coarser numerical mesh over a range of different localized heating scenarios (representing the urban heat island effects), and for different values of Rayleigh numbers, $10^7 \leq Ra \leq 10^9$.

2. Governing equations

The transport of mass, momentum, and heat in the turbulent thermal convection in the Large-Eddy Simulation (LES) approach are represented by the spatially-averaged (filtered) transport

Journal of Physics: Conference Series **2766** (2024) 012055 doi:10.1088/1742-6596/2766/1/012055

equations that can be written as:

$$\frac{\partial u_i}{\partial x_i} = 0 \tag{1}$$

$$\frac{\partial u_i}{\partial t} + \frac{\partial (u_i u_j)}{\partial x_j} = -\frac{1}{\rho_0}\frac{\partial p}{\partial x_i} + \frac{\partial}{\partial x_j}\left[\nu\left(\frac{\partial u_i}{\partial x_j} + \frac{\partial u_j}{\partial x_i}\right) - \tau_{ij}\right] - g_i\beta\left(\theta - \theta_0\right) \tag{2}$$

$$\frac{\partial \theta}{\partial t} + \frac{\partial (\theta u_j)}{\partial x_j} = \frac{\partial}{\partial x_j}\left(D_\theta \frac{\partial \theta}{\partial x_j} - \tau_{\theta j}\right) \tag{3}$$

where ρ_0 is density of fluid at reference temperature (θ_0), β is thermal expansion coefficient, D_θ is molecular thermal diffusion, and, finally, τ_{ij}, and $\tau_{\theta j}$ are sub-grid turbulent stress tensor, and sub-grid turbulent heat flux, respectively, that need to be modeled. Here, we apply the eddy-viscosity closure for sub-grid turbulent stress tensor and a simple-gradient diffusion hypothesis (SGDH) for the sub-grid turbulent heat flux vector:

$$\tau_{ij}^{LES} = -\nu_t^{SGS}\left(\frac{\partial u_i}{\partial x_j} + \frac{\partial u_j}{\partial x_i}\right) + \frac{1}{3}\tau_{kk}\delta_{ij}, \quad \tau_{\theta j}^{LES} = -\frac{\nu_t^{SGS}}{Pr_T^t}\frac{\partial \theta}{\partial x_j} \tag{4}$$

where we adopted the following closure of [10], which performed well in comparison to the DNS results in our previous work dealing with non-stratified turbulent thermal convection over flat and differently shaped heated surfaces, [11]:

$$\nu_t^{SGS} = c_{SGS}\sqrt{\frac{B_\beta}{\alpha_{ij}\alpha_{ij}}}, \ \alpha_{ij} = \frac{\partial u_i}{\partial x_j}, \ \beta_{ij} = \Delta_m^2 \alpha_{mi}\alpha_{mj},$$
$$B_\beta = \beta_{11}\beta_{22} - \beta_{12}^2 + \beta_{11}\beta_{33} - \beta_{13}^2 + \beta_{22}\beta_{33} - \beta_{23}^2 \tag{5}$$

with a sub-grid model coefficient $c_{SGS} = 0.07$, Δ_m as the control volume filter-length projections in particular coordinate directions, and $Pr_T^t = 0.4$.

In addition to the wall-resolved high-resolution LES, we also introduced the time-dependent Reynolds-Averaged Navier-Stokes (TRANS) approach based now on the time-averaged (instead of the spatially averaged) governing transport equations, [12–14]. Here, we applied the 3-equation $k - \varepsilon - \overline{\theta^2}$ turbulence model, where k is the turbulent kinetic energy, ε is the dissipation rate, and finally, $\overline{\theta^2}$ is the temperature variance, [12]. Furthermore, the algebraic form of the turbulent heat flux model (AFM) is used:

$$\tau_{\theta i}^{TRANS} = -C_\theta \frac{k}{\varepsilon}\left(\tau_{ij}^{TRANS}\frac{\partial \overline{T}}{\partial x_j} + \xi \tau_{\theta j}^{TRANS}\frac{\partial \overline{U_i}}{\partial x_j} + \eta\beta g_i \overline{\theta^2}\right) \tag{6}$$

where the model coefficients are: $C_\theta = 0.2$, $\xi = 0.6$, $\eta = 0.6$, [12]. Finally, instead of using a direct-integration up to the wall as in the LES, in TRANS approach we use the buoyancy extended wall functions of all transport (i.e. velocity, temperature, and turbulence parameters) variables, [15].

3. Numerical method

The discretized forms of above defined governing equations (for both the LES and TRANS) are solved by our in-house finite-volume code for general non-orthogonal structured geometries, [11–14]. The collocated grid arrangement is applied for all transport (PDEs) variables. The SIMPLE algorithm is used to solve the pressure field. For the LES, both convective and diffusive terms of all transport equations are calculated by the central-differencing scheme (CDS). For the TRANS, all diffusive terms are discretized by the CDS-scheme, whereas the convective terms are represented by the second-order linear-upwind (LUDS) scheme. For both, LES and TRANS, the fully implicit second-order time integration scheme is applied, [11].

Journal of Physics: Conference Series **2766** (2024) 012055 doi:10.1088/1742-6596/2766/1/012055

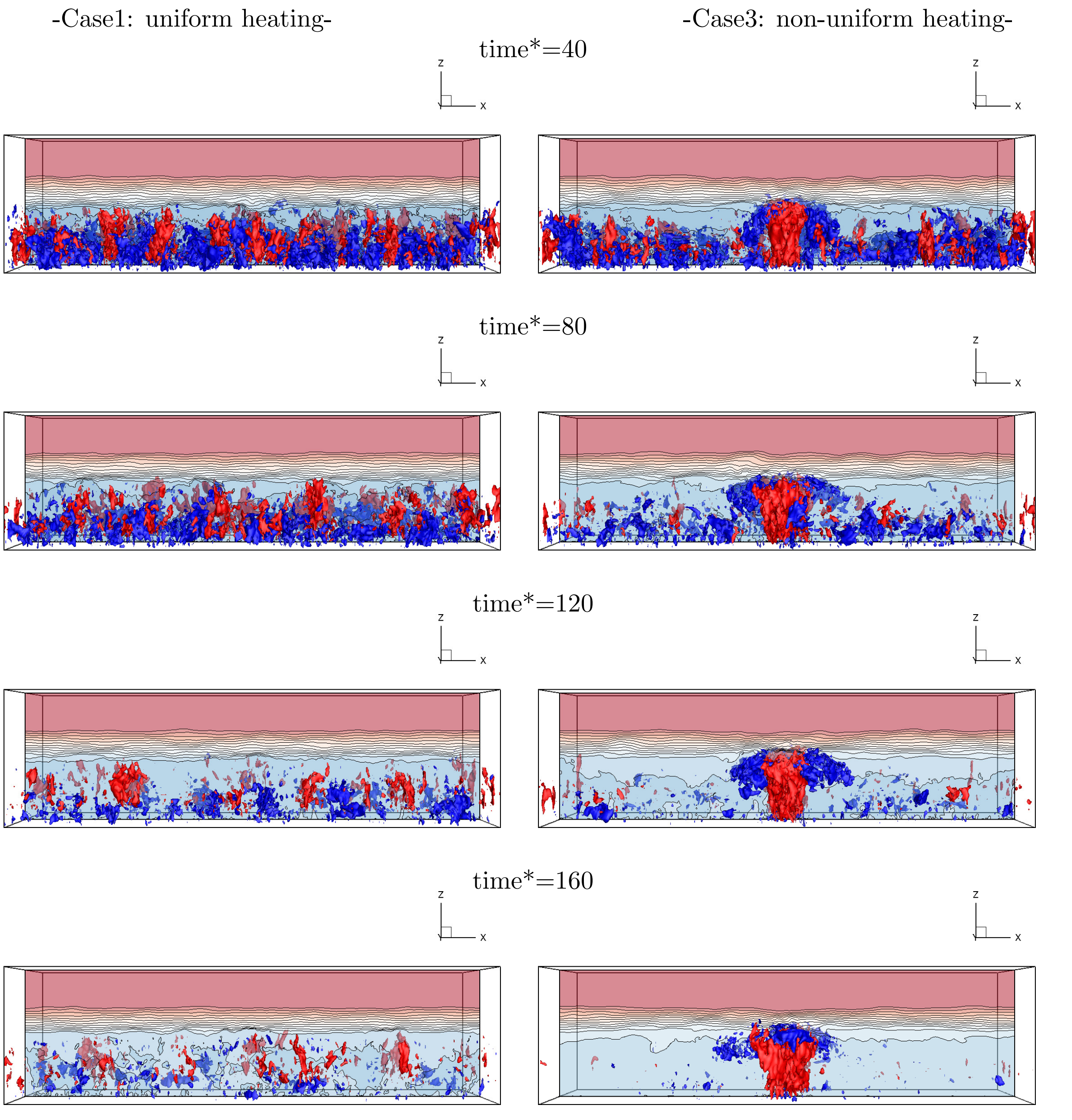

Figure 1. Time-evolution of convective structures (selected as iso-surfaces of instantaneous non-dimensional vertical velocity, $w^* > 0$ - red, $w^* < 0$ - blue), and background levels of the instantaneous temperature in the central vertical plane for cases with uniform (Case1) and non-uniform (Case3) heating scenarios - both with LES at $Ra = 10^9$.

4. Geometry, boundary conditions and numerical mesh

The simulated computational domain is represented by a $0 \leq x/L \leq 9$, $0 \leq y/W \leq 4$, $0 \leq z/H \leq 2.5$ volume with local mesh refinements in the proximity of the ground and vertical locations of the imposed initial thermal stratification. The temperature inversion layer is starting at $z/H = 1$ and ending at $z/H = 2$, with a non-dimensional gradient of $\partial T^*/\partial z^* = 4$ (mimicking

Journal of Physics: Conference Series **2766** (2024) 012055 doi:10.1088/1742-6596/2766/1/012055

a strong thermal stratification in the atmosphere). The upper stress-free boundary condition is kept at the constant temperature ($T^*_{top} = 4$). The side boundaries are kept as the no-slip for velocity and zero-gradient for turbulence parameters. Various heating scenarios are applied at the ground, varying from the uniform heating ($T^*_{bottom} = 1$), and in addition, with superimposed local heating sources representing the urban heat islands (UHI) of various extensions (e.g. Case3, representing a 2D UHI, with $T^*_{UHI} = 2$ distributed over $4 \leq x/L \leq 5$ and $0 \leq y/W \leq 4$ or Case7, distributed over $4 \leq x/L \leq 5$ and $1.5 \leq y/W \leq 2.5$). Various values of the representative Rayleigh number are simulated, $10^7 \leq Ra \leq 10^9$, with a fixed $Pr = 0.71$. The final numerical mesh for LES contains $Nx \times Ny \times Nz = 362 \times 102 \times 242$ control volumes (CVs), whereas TRANS uniformly distributed mesh is significantly coarser, with $Nx \times Ny \times Nz = 60 \times 60 \times 60$ CVs. The locations of the wall-nearest grid points are $z/H_{inv} = 2.5 \times 10^{-4}$ for the LES and $z/H_{inv} = 2.0 \times 10^{-2}$ for the TRANS, where H_{inv} is the initial height of the inversion zone.

5. Results and discussion

We start the discussion of results by analyzing the time-evolution of typical convective structures in the region between the ground and the start of the inversion zone, figure 1. Here we select iso-surfaces of positive and negative non-dimensional vertical velocity (w^*) to characterize typical updrafts and downdrafts, respectively. For the uniform heating scenario, there is a random distribution of intermittent convective structures, which strength slowly decreases with time due to an intensive turbulent mixing and suppressing effect of the capping inversion layer. In contrast, for the non-uniform heating scenario (which represents a heat urban island effect), there is a distinct central updraft extending to the start of the inversion layer, even at the latter time instants. For each of the simulated scenarios, we also perform simulations based on the TRANS approach. The main objective is to conduct a direct comparison with the LES results. The characteristic thermal plume structures (identified as an iso-surface of the instantaneous temperature colored by the vertical velocity) for LES and TRANS are shown in figure 2. It can be seen that a reasonable agreement between the most dominant thermal plume structures is present for both cases, whereas the TRANS (as expected) is not capturing the fine structures. Note that the present TRANS numerical mesh is just 2.5% of the total mesh elements used in the referent LES.

Next, we directly compare time evolutions of the horizontally averaged inversion height and the mean temperature profiles obtained by LES and TRANS for a uniform heating scenario, and two values of $Ra = 10^7, 10^9$, respectively, figure 3(a). It can be seen that the agreement is good for both values of Rayleigh number, i.e. the dynamics of the elevation height of the capping inversion layer is well captured by the TRANS. It should be noted that the TRANS simulations with a simple-gradient diffusion hypothesis (SGDH) model for the turbulent heat flux deviated significantly from the LES profiles, figure 3(b) stressing the importance of a proper representation of the all main production mechanisms of the sub-scale turbulent heat flux. Finally, the vertical profiles of the horizontally averaged non-dimensional temperature (θ^*) exhibit an overall good agreement for both $Ra = 10^7$ and 10^9, with some small deviations in the initial mixing phase ($\theta^* = 20$).

6. Conclusions

By performing a series of numerical simulations with LES and TRANS methods for turbulent heat transfer of penetrative convection in a stable stratification, we concluded that overall good agreement was obtained in representing the most dominant convective structures as well as in predicting time evolutions of the horizontally averaged temperature profiles. These findings confirm the potential of the TRANS approach in various environmental applications characterized by high values of Rayleigh numbers, as well as complex urban areas capped by stable thermal stratification.

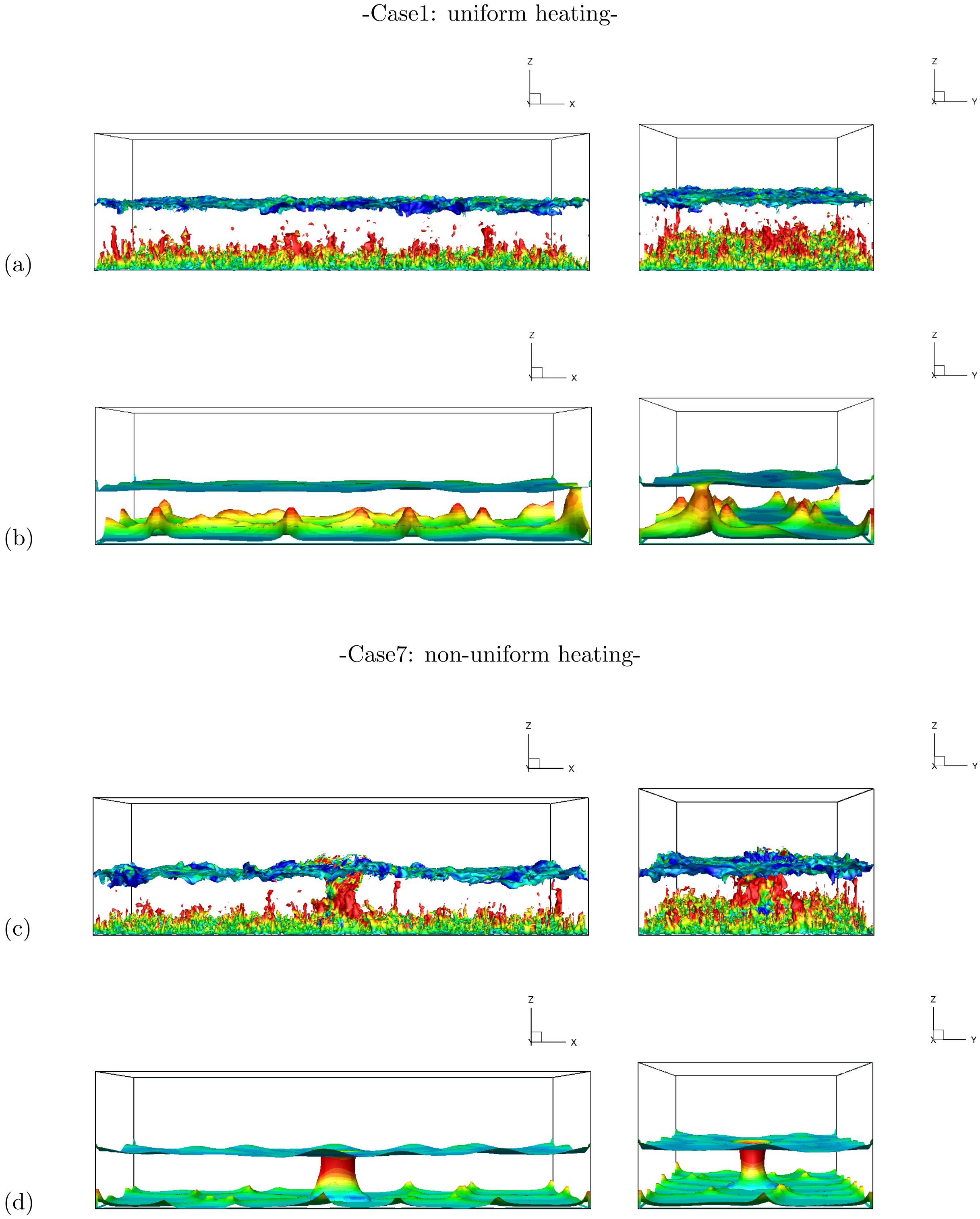

Figure 2. Iso-surface of the instantaneous non-dimensional temperature (θ^*) at characteristic non-dimensional time of $t^* = 200$, with two heating scenarios: Case1- uniform and Case7- nonuniform heating: (a) and (c) - LES results; (b) and (d) - TRANS (AFM) results; Left- a view in (x-z) plane; Right- a view in (y-z) plane;

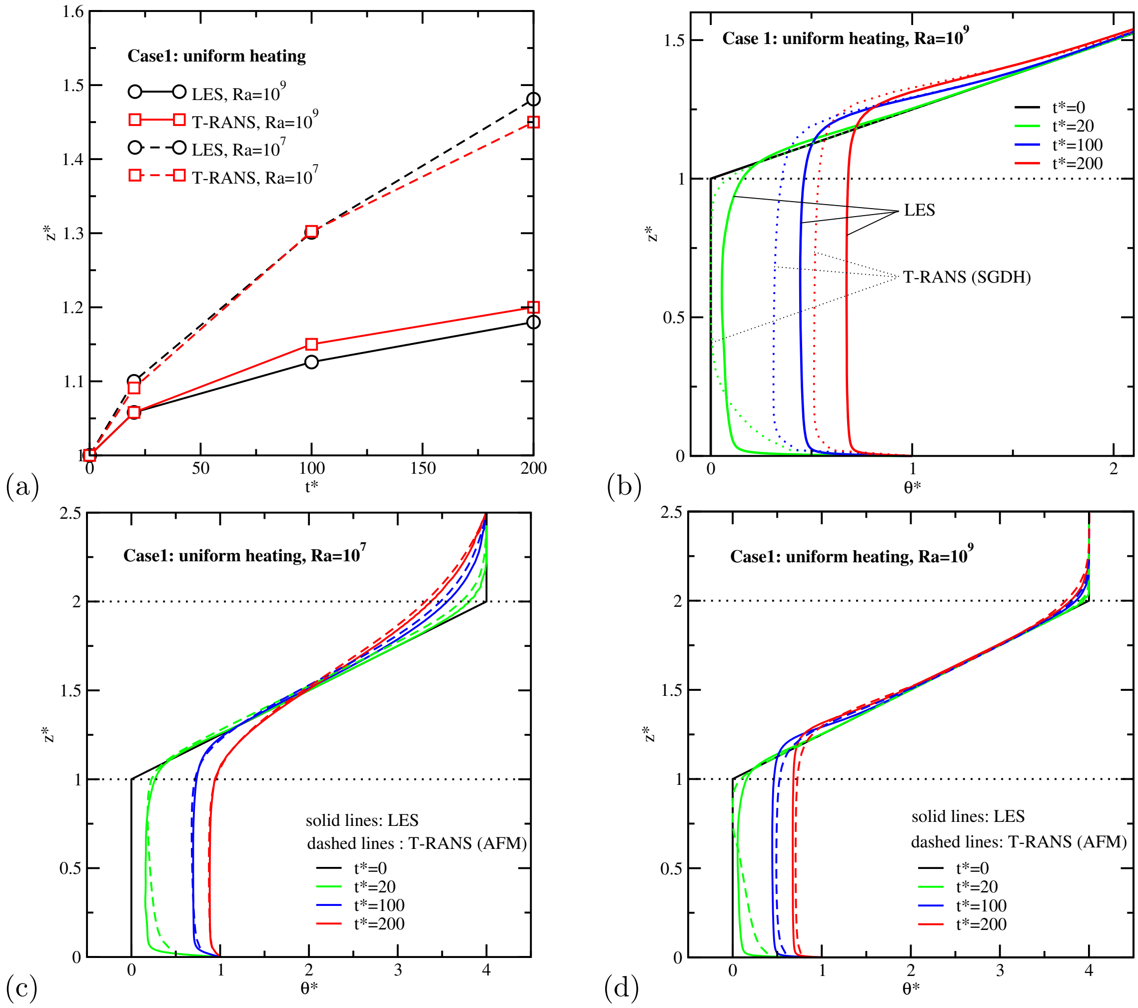

Figure 3. The progression of the height of the inversion base with time for the Case1 (uniform heating in an initially stable stratification) at $Ra = 10^7$ and $Ra = 10^9$ (a); The TRANS results for the uniform heating case (Case1) at $Ra = 10^9$ with SGDH for the turbulent heat flux (a zoom-in) (b). The time evolution of the non-dimensional horizontally-averaged temperature (θ^*) profiles for the Case1 at $Ra = 10^7$ (c) and $Ra = 10^9$ (d).

References

[1] Deardorff J W, Willis G E, Lilly D K 1969 *J. Fluid Mech.* **35** (1), 7–31
[2] Kurbatskii A F 2001 *J. Appl. Meteorol.* **40**, 1748–1761
[3] Kenjereš S, Hanjalić K 2002 *Journal of Turbulence* **3** (1) 026, 1–25
[4] Fedorovich E, Conzemius R, Mironov D 2004 *J. Atmos. Sci.* **61**, 281–295
[5] Basu S, Porté-Agel F 2006 *J. Atmos. Sci.* **63**, 2074–2091
[6] Kurbatskii A F, Kurbatskaya L I 2009 *Meteorol. Atmos. Phys.* **104**, 63–81
[7] Abkar M, Moin P 2017 *Boundary Layer Meteorology* **165** (3), 405–419
[8] Stoll R, Gibbs J A, Salesky S T, Anderson W, Calaf M 2020 *Boundary-Layer Meteorology* **177**, 541–581
[9] Chinita M J, Matheou G, Miranda P M A 2022 *Quart. J. Royal Meteorological Society* **148**, 1805–1823
[10] Vreman A W 2004 *Phys. Fluids* **16**, 3670–3681
[11] Kenjereš S 2015 *Physical Review E* **92** (5), 053006, 1–14
[12] Kenjereš S, Hanjalić K 1999 *Int. J. Heat and Fluid Flow* **20** (3), 329–340
[13] Kenjereš S, Hanjalić K 2006 *Int. J. Heat and Fluid Flow* **27** (5), 800–810
[14] Kenjereš S, Hanjalić K 2009 *Fluid Dynamics Research* **41** (1), 012201, 1–32
[15] Hanjalić K., Hrebtov M. 2016 *Boundary-Layer Meteorology* **160**, 41–61